Magnetic and electrostatic fluctuations in the CASTOR tokamak

1999 Plasma Phys. Control. Fusion 41 A577

(http://iopscience.iop.org/0741-3335/41/3A/051)

Plasma Phys. Control. Fusion **41** (1999) A577–A585. Printed in the UK PII: S0741-3335(99)97516-4

Magnetic and electrostatic fluctuations in the CASTOR tokamak

J Stöckel†, J Badalec†, I Ďuran†, M Hron†, J Horáček†, K Jakubka†, L Kryška†, J Petržílka†, F Žáček†, M V P Heller‡, Z A Brazilio‡ and I L Caldas‡

† Institute of Plasma Physics, Academy of Sciences of the Czech Republic, Prague, Czech Republic
‡ Institute of Physics, University of Sao Paulo, Sao Paulo, Brazil

Received 3 July 1998

Abstract. Magnetic and electrostatic fluctuations are measured in the CASTOR tokamak with a reasonable spatial and temporal resolution to better understand the nature of turbulent processes in tokamaks. We have found that the broadband magnetic fluctuations in the plasma core are nearly independent of the safety factor $q(a)$. However, their level is dramatically reduced (by a factor of three) when the aspect ratio increases from 5.4 to 6.6. The character of electrostatic structures in the edge plasma was found to be quite similar to that observed in large tokamak experiments. Furthermore, the fluctuations of the longitudinal current have been identified in the scrape-off layer. These fluctuations might represent a link between the magnetic and electrostatic components of plasma turbulence in this region.

1. Introduction

Knowledge of the plasma turbulence in tokamaks is still incomplete and, evidently, spatially resolved measurements of plasma fluctuations are necessary to characterize the turbulent structures and to understand better their nature. In general, the turbulent structures formed in toroidal devices are three-dimensional objects. In particular, the poloidal component of electrostatic fluctuations and the radial component of magnetic fluctuations are of importance for radial particle/energy transport. This is seen, for example, from the well known expression for the radial particle flux induced by fluctuations

$$\tilde{\Gamma} \sim \frac{\langle \tilde{n} \tilde{E}_{\mathrm{p}} \rangle}{B_{\mathrm{t}}} + v_{\parallel} \tilde{B}_{\mathrm{r}} / B_{\mathrm{t}}.$$

One of the efficient diagnostic tools, namely at the plasma edge, are the arrays of probes having a reasonable spatial resolution. Spatially resolved measurements of electrostatic fluctuations, performed recently on the ASDEX tokamak and the W7-AS stellarator with a poloidal probe array, have led to the formulation of the concept of 'eddies' [1, 2]. The radial component of magnetic fluctuations was studied not only at the plasma edge but also in the confinement region of the Tokapole tokamak [3] and the CHS heliotron/torsatron [4].

Systematic measurements of plasma fluctuations by using probe arrays are performed on the CASTOR tokamak to compare the edge turbulence in large-[1, 2] and small-size experiments. Results of electric probe measurements at the plasma edge are presented in [5, 6], while details of magnetic measurements in the core plasma are described in [7]. The

0741-3335/99/SA0577+09$19.50

aim of this contribution is to summarize the main results achieved there and, in addition, to present the first results of current fluctuation measurements in the scrape-off layer (SOL) of the CASTOR tokamak.

2. Experimental arrangement

Experiments were carried out on the CASTOR tokamak ($R = 0.4$ m) with the circular cross section of the plasma column. The minor radius is fixed by a poloidal limiter $a = 0.085$ m. Optionally, an additional material limiter with $a = 0.06$ m can be introduced into the vacuum chamber to enhance the aspect ratio. The safety factor $q(a)$ is varied in a rather broad range, $q(a) = 2.8$–15 ($B_t = 0.5$–1.2 T, $I_p = 5$–15 kA). The line-averaged density is kept around $\bar{n} = 0.8$–1.0×10^{19} m^{-3}, the central electron temperature being in the range of 150–250 eV. The position of the plasma column is feedback-stabilized both in the horizontal and vertical directions. Magnetic and electrostatic fluctuations are monitored by the probe arrays schematically shown in figure 1.

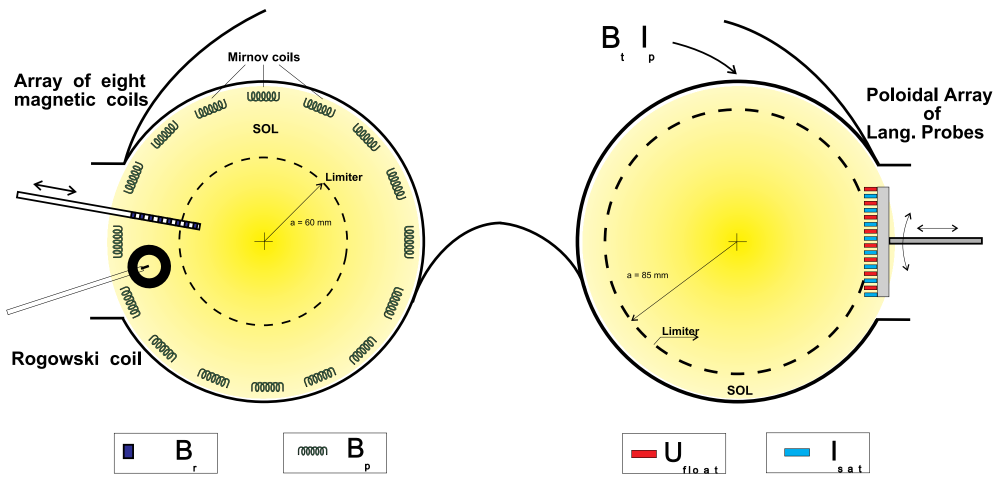

Figure 1. Experimental layout of the probe diagnostics on the CASTOR tokamak. Besides the diagnostics reported here (as the radial array of B_r-probes, poloidal array of Langmuir probes and Rogowski coil), the 16 Mirnov coils, located in the limiter shadow are also depicted.

The B_r component of magnetic fluctuations is measured by the radial array of eight absolutely calibrated magnetic probes with the spatial resolution 6.7 mm. The total active length of the probe array represents more than 50% of the plasma minor radius. The probe signals are sampled at a rate of 0.2 μs/sample and integrated numerically. The low frequencies (<10 kHz) are removed numerically, the high frequencies (>300 kHz) are filtered out by passive integrators to avoid aliasing.

Electrostatic fluctuations are monitored by a poloidal array of 16 Langmuir probes spaced by 2.5 mm. The odd tips are biased (−100 V) to measure the ion saturation current, while the even tips monitor the floating potential (see figure 1). Neglecting electron temperature fluctuations, this allows us to measure density and potential fluctuations with a spatial resolution of about 5 mm and to study the correlation between them. The frequency band of electrostatic measurements is 1.5–150 kHz, the sampling is 1 μs. The radial position of the probe array can be changed on a shot-to-shot basis and, if necessary, inclined poloidally by $\pm 25^\circ$ to adjust all the tips to a single magnetic surface as close as possible. The respective position of the poloidal probe array and a magnetic surface is checked by measuring the profile of the time averaged floating potential along the probe array.

Fluctuations of toroidal plasma current are measured by a small Rogowski coil with the spatial resolution 7 mm. Plasma parameters inside the Rogowski coil cross section are measured by the single Langmuir probe. Additional details are given in section 3.4.

3. Experimental results

3.1. Magnetic fluctuations

The frequency spectrum of B_r-fluctuations, in discharges with $q(a) < 7$, is typically a superposition of the two components, as shown in figure 2. There is a broadband component characterized by the power spectrum decaying with frequency as f^{-2}. The second component, a relatively narrow peak ($\Delta f \approx 10$ kHz) appearing at frequencies 50–100 kHz, was identified as a coherent magnetohydrodynamic MHD mode with the poloidal mode number $m = 2$, rotating in the poloidal plane [7, 8]. In high q-regimes ($q(a) > 7$), only the broadband component is observed.

Correlation analysis of the broadband fluctuations can be performed only in the frequency bands, which are not influenced by the coherent mode. We have found that the radial correlation length of the broadband fluctuations is about 1.5 cm, which is much shorter than the correlation length of the coherent fluctuations. Moreover, their radial propagation in the outward direction seems to be identified.

To derive the level of the broadband component, we suppress numerically the spectrum in the frequency band corresponding to the coherent peak. The removed part of the spectrum is interpolated by the broadband component as sketched in figure 2. The root mean square value (RMS) of the broadband component is plotted against the normalized radius in figure 3 for the two values of the aspect ratio. Each radial profile of B_r-fluctuations averages data from about

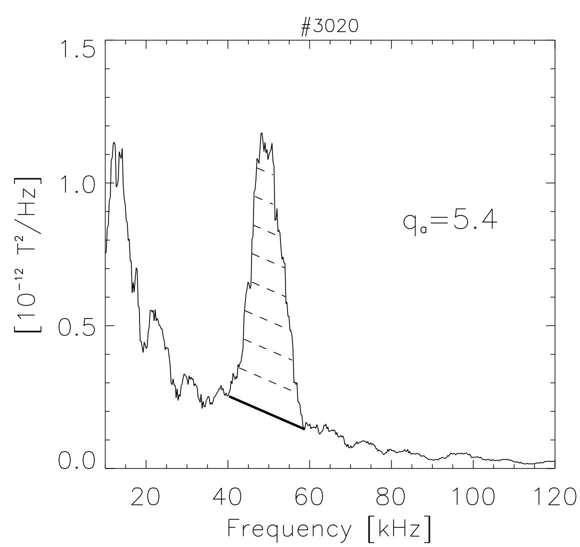

Figure 2. Typical power spectrum of B_r-fluctuations measured in a discharge with $q(a) = 5.4$ by the most inner probe located at $r/a = 0.63$.

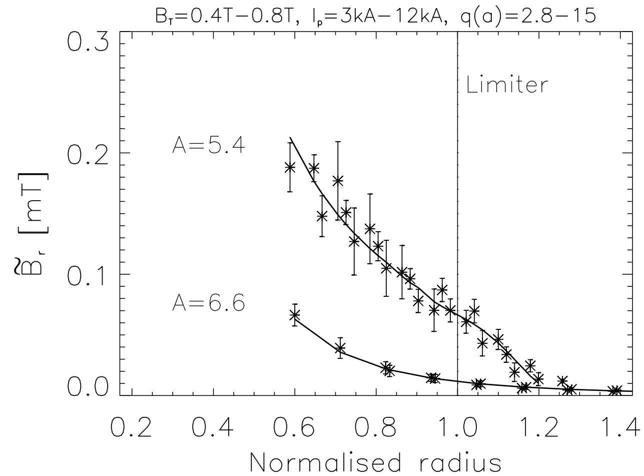

Figure 3. Radial profiles of B_r-fluctuations in the CASTOR tokamak for two values of the aspect ratio, $A = 6.6$ and $A = 5.4$. Each profile is averaged over ∼70 shots with a broad range of safety factors $q(a) = 2.4$–15. The line-averaged density is kept between 0.8–1 × 10^{19} m^{-3}.

70 shots with a rather broad range of the safety factors ($q(a)$ from 2.8 to 15). It is apparent that the form of the radial profile is nearly independent on q for the given value of the limiter radius. On the other hand, the level of B_r is reduced by a factor of three, if the limiter radius was reduced from $a = 85$ mm to $a = 60$ mm: the aspect ratio increases from $A = 5.4$ to $A = 6.6$.

3.2. Electrostatic fluctuations at the plasma edge

Typical examples of the spatial-temporal evolution of signals from the poloidal probe array monitored in the limiter shadow are shown in figure 4. Spatially and temporally localized structures of density and potential, their poloidal propagation as well as their mutual relation are clearly apparent. To find quantitative information, several statistical methods have been used for analysis of these fluctuations. For example, calculations of the probability density function (PDF) of the probe signals have shown that the PDF of the ion saturation current fluctuations deviates definitely from the Gaussian distribution more than the PDF of the potential fluctuations [8]. This might indicate the existence of coherent structures in plasma density. Similar conclusions can be drawn from other statistical techniques, such as wavelet bicoherence and conditional analysis, as will be described in [9] in more detail.

The main results of the correlation analysis of the electrostatic fluctuations are briefly summarized as follows. We find that the poloidal correlation length (1–2 cm) and the correlation time (10–20 μs) of the density as well as the potential structures in the SOL are nearly independent of discharge parameters. In addition:

- both the density and potential fluctuations reveal a periodicity in the poloidal direction; the typical poloidal wavelength is in the range 10–15 cm, the potential structures seem to be systematically longer in the poloidal direction (by ∼10%) than the density ones;
- there is a mutual correlation between the potential and density; in particular, the poloidal electric field E_p, proportional to the differential signal from two adjacent floating probes, is highly correlated with the signal of the ion saturation current measured between them, the correlation coefficient $C_{nE_p} = 0.65$–0.85.

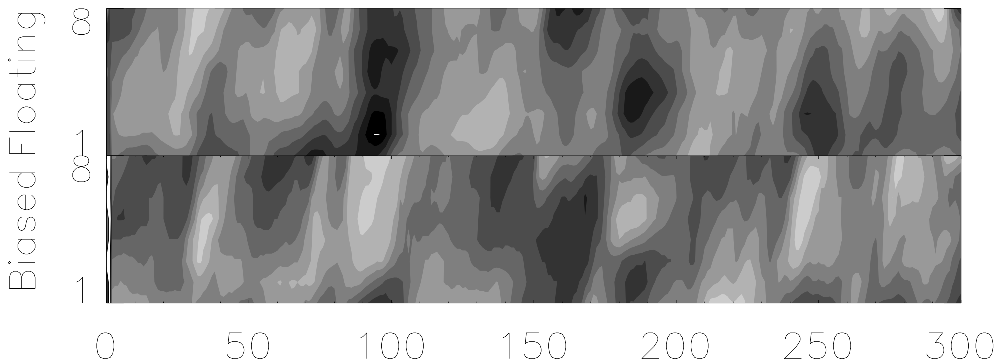

Figure 4. 2D plot of data from the poloidal probe array. Top panel — floating potential (∼plasma potential). Bottom panel — ion saturation current (∼plasma density). The horizontal axis of each panel represents the time interval 300 μs, the vertical axis corresponds to the poloidal length of the probe array (35 mm). Bright regions indicate an enhanced level of potential (density) and *vice versa*.

All the results of the correlation analysis of potential and density fluctuations in the SOL on the CASTOR tokamak are comparable with those from ASDEX. This may indicate a universal nature of the electrostatic turbulence at the plasma edge, independently of the size of the experiment. Some exceptions, observed in the vicinity of the velocity shear layer in regimes with a higher aspect ratio, are presented in [5].

3.3. Model of eddies

Our observations are nearly consistent with the model of eddies proposed in [1]. This model is based on the concept of the flute-like instability having positive increment in the SOL at the low-field side of the torus with unfavourable curvature of the magnetic field lines. The theoretical basis was proposed by Nedospasov [10], Garbet *et al* [11] and recently specified quantitatively for ASDEX geometry by Endler *et al* [1].

Without going into the details of the mechanism of the flute-like instability, we point out some features important for this experiment using the schematic picture seen in figure 5. The picture represents a snapshot of two potential structures (tubes) having potentials above and below a mean value, which are formed in the limiter shadow. They are assumed to be long, i.e. their parallel wavenumbers are much less than the perpendicular ones ($k_\parallel \ll k_{\mathrm{p}}$, k_{r}) as found in [6], thus they terminate at the limiter.

An important consequence of this model is that the potential of the structures is equilibrated by currents flowing through the limiter surface. Since the current fluctuations have not yet been measured in tokamaks, we summarize their *expected* characteristic features to have a basis for the design and the interpretation of our experiments.

• ‘Current filaments’ should be of the same dimensions and localized at the same places as the potential structures. Consequently, a significant correlation between both of them is expected in the SOL. The sign of the correlation coefficient between current and potential should be opposite at the electron and the ion side of the limiter.

• The amplitude of the current fluctuations should reach a maximum near the limiter surface. On the other hand, the level of current fluctuations should be close to zero at some point away from the limiter (in the symmetric case this would be at the toroidal position opposite to the limiter).

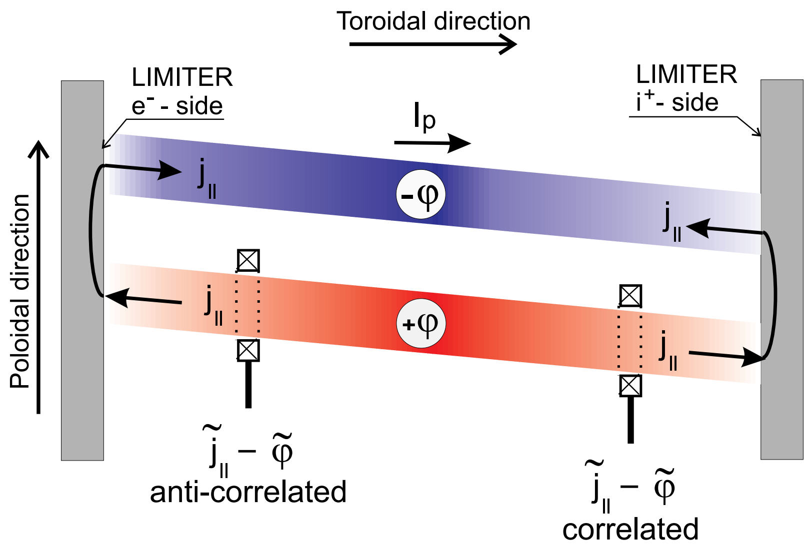

Figure 5. Formation of current tubes on a particular magnetic surface in the SOL as unfolded to the plane. The major circumference is plotted horizontally and plugged by the electron and ion sides of the poloidal limiter. The vertical axis corresponds to the poloidal circumference. The two toroidal positions of the measuring element (Rogowski coil) are also depicted.

• The current density within the current structure should be of the order of the ion saturation current density [1].

• The amplitude of the magnetic fluctuations in the SOL must be proportional to the amplitude of the current fluctuations.

The lifetime, poloidal dimensions and mutual distance of the potential tubes can be deduced from the correlation analysis of data from the poloidal probe array. The next section is devoted to a description of direct measurements of the current/potential fluctuations performed to check the Nedospasov–Endler model.

3.4. Current fluctuations in the plasma edge

To measure the current fluctuations in the plasma edge, a small Rogowski coil (RC) was designed and constructed. The inner diameter of RC, chosen as $d = 7$ mm, is a compromise between the expected size of the current structures (1–2 cm), a reasonable spatial resolution and construction limits. Toroidally near the RC ($\sim$5 mm), a single Langmuir probe (LP) was installed to measure a possible correlation of the current and potential (density) fluctuations. Both the RC and LP are fixed on the same arm, movable in the radial direction on the shot-to-shot basis.

In reality, the RC detects not only currents flowing through its cross section, but it is also sensitive to magnetic perturbations having their origin outside. To distinguish the signal related to current flowing through the RC cross section from such a noise, the RC is equipped by two movable protecting plates. The noise level is determined in discharges in which the active area of the RC is closed by these protecting plates (see figure 6).

Results of preliminary experiments are shown in figure 7. In this experimental series, the combined (RC + LP) probe is inserted horizontally into the edge plasma from the low-field

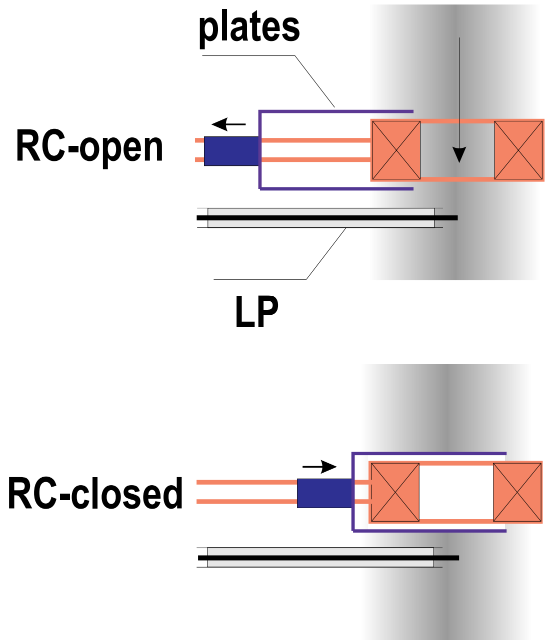

Figure 6. Rogowski coil with the protecting plates. The two positions of the protecting plates allow us to distinguish between the useful signal and background noise in two subsequent shots.

side, a few degrees toroidally away from the ion side of the material limiter. The left column of figures shows radial profiles measured by the combined probe, when the Langmuir probe was floating. The profiles in the right column are obtained with the LP in the ion saturation current regime.

The radial profile of the time-averaged floating potential is shown in the left top figure. The observed maximum of the floating potential is attributed to the radial position of the last closed flux surface (LCFS). As seen, the LCFS is not identical with the radius of the main poloidal limiter ($a = 85$ mm) for this shot series. This is a result of an inward shift of the plasma column, which is pre-programmed by the feedback system of the CASTOR experiment. Consequently, the magnetic field lines located between the LCFS and material limiter still terminate at the material surface, but after a few circumnavigations around the torus. The horizontal scale in figure 7 is normalized with respect to the position of the LCFS.

The middle left figure shows the radial profile of the current fluctuations. We see a plateau on the $j_\parallel$-profile just outside the LCFS with $j_\parallel = 0.3$ A cm^{-2}, which is well above the background noise. The level of current fluctuations increases much more steeply in the direction towards the plasma core where the magnetic field lines do not terminate at the limiter. Note that the level of current fluctuations is negligible in the geometrical shadow of the material limiter.

Similar results were obtained in the next shot series (with similar discharge parameters) with the Langmuir probe operating in the regime of the ion saturation current. The radial profile of density fluctuations (right upper panel), measured by the Langmuir probe looks similar to that of the current fluctuations, with the exception of the geometrical shadow of the material limiter, where the radial profile of the current fluctuations decays more steeply than the density fluctuations.

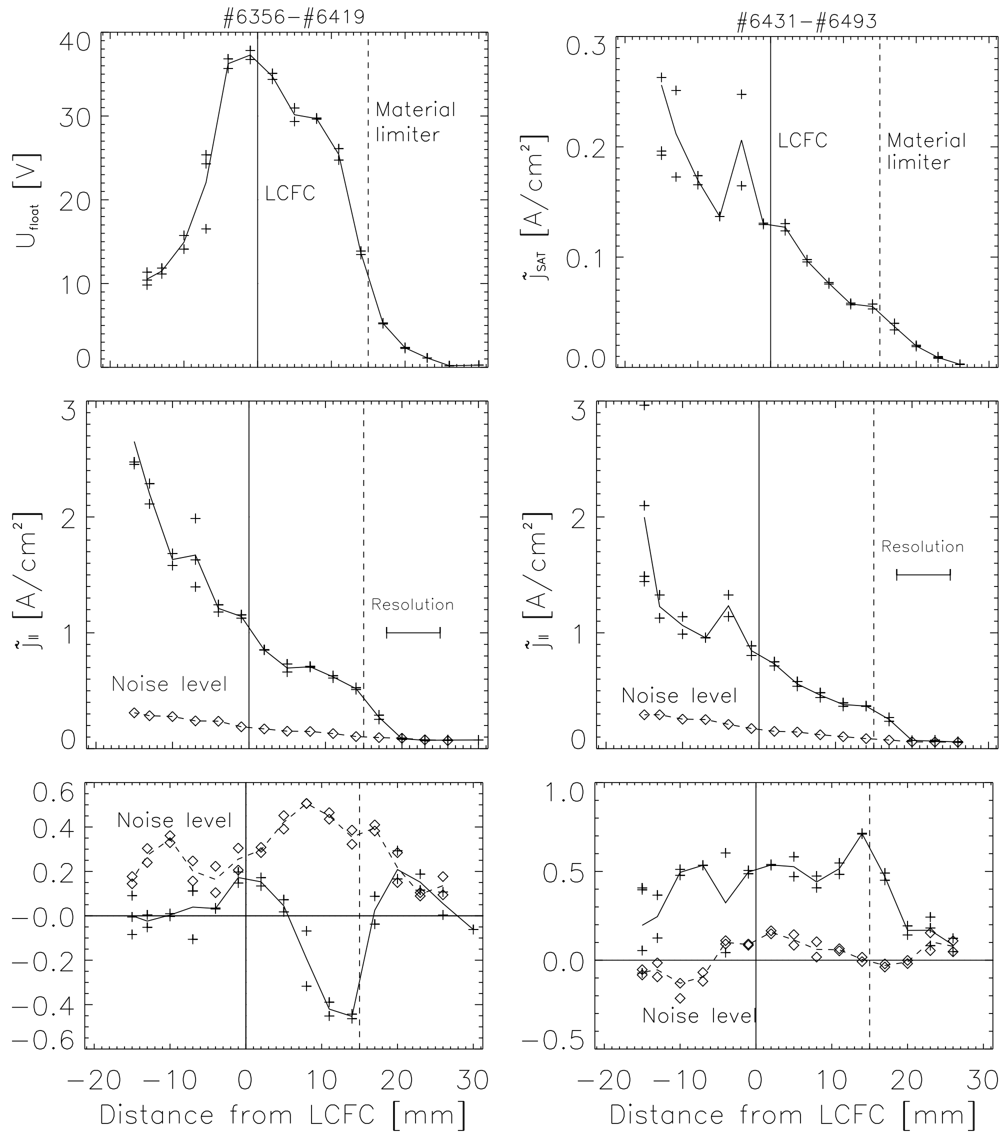

Figure 7. Radial profiles measured in two series of shots by the combined (RC + LP) probe. The horizontal axis represents the normalized distance from the LCFS. LP is floating (left column from top to bottom): time-averaged floating potential, current fluctuations, correlation coefficient between the longitudinal current and potential fluctuations. LP is biased (right column from top to bottom): density fluctuations (from the ion saturation current), current fluctuations measured by the RC, correlation coefficient between the longitudinal current and density fluctuations.

The bottom panels of figure 7 show the radial profiles of the correlation coefficient between the current fluctuations and potential/density fluctuations, respectively. We see the following.

• The correlation coefficient $C_{j\phi}$ differs significantly from the noise level just in the region between the LCFS and material limiter, i.e. in the region where the magnetic field lines are of a finite length but still longer than the circumference of the torus. The $j - \phi$ correlation is comparable with the noise level in the shadow of the material limiter.

It is necessary to note that the correlation between the current and potential is relatively high in the whole investigated region, even if the RC is closed by the protecting plates. This experimental observation is not yet well understood.

• The correlation coefficient between the current and density fluctuations is relatively high and well above the noise level in the whole range of radii, except in the shadow of the material limiter.

4. Summary

Experiments performed on the CASTOR tokamak have shown that the character of electrostatic fluctuations in the edge plasma is similar to that observed in large-scale experiments. In particular, the scale lengths and lifetimes of electrostatic structures are nearly the same as on ASDEX. This might indicate a universal nature of plasma turbulence in tokamaks.

One of the possible models explaining the observed features of edge electrostatic turbulence is based on the flute-like instability in the scrape-off plasma. This model predicts fluctuations of the longitudinal current in the scrape-off plasma. Such current fluctuations have been identified on the CASTOR tokamak for the first time, using a small RC and their correlation with the electrostatic fluctuations has been observed. The basic features of the model seem to be confirmed. However, a more detailed comparison needs further experiments. In particular, we plan to measure the sign of the $j_{\parallel} - \phi$ correlation in the scrape-off plasma at different respective positions of the RC and limiter surface (in the toroidal direction), knowing details of the magnetic configuration in this region.

The radial component of the broadband magnetic fluctuations in the plasma column was found to be independent of the safety factor $q(a)$, but is reduced when the aspect ratio increases.

Acknowledgments

This work was performed with support of grants from the Academy of Sciences of the Czech Republic Nos IAA1043701 and KSK1043601. The authors are indebted to K Dyabilin for useful comments to the manuscript.

References

[1] Endler M, Niedermayer H, Giannone L, Holzhauer E, Rudyj A, Theimer G, Tsois N and the ASDEX Team 1995 *Nucl. Fusion* **35** 1307
[2] Bleuel J, Endler M, Niedermeyer H and Theimer G 1997 *Proc. 24th EPS Conf. on Control. Fusion and Plasma Phys. (Berchtesgaden 1997)* vol 4, p 1613
[3] Graessle D E, Prager S C and Dexter R N 1991 *Phys. Fluids* B **3** 2626
[4] Oike T, Toi K, Ohdachi S, Sakibara S, Marisaki P, Miami T, Tanaka K, Morita S, Okamura S and Matsuoka K 1996 *Proc. 1996 Int. Conf. on Plasma Physics (Nagoya 1996)* vol 1, p 346
[5] Stöckel J, Dhyani V, Jakubka K, Kryška L, Žáček F, Ďuran I, Hron M and Petržílka J 1997*Proc. 24th EPS Conf. on Control. Fusion and Plasma Phys. (Berchtesgaden 1997)* vol 1
[6] Petržílka J and Stöckel J 1997 *Contrib. Plasma Phys.* **38** 74
[7] Ďuran I, Stöckel J and Jakubka K 1998 *Proc. 1998 Int. Congress on Plasma Phys. (Prague 1998)* p 714
[8] Stöckel J *et al* 1996 *Proc. 1996 Int. Conf. on Plasma Phys. (Nagoya 1996)* vol 1, p 322
[9] Heller M V P *et al Plasma Phys. Control. Fusion* submitted
[10] Nedospasov A V 1989 *Sov. J. Plasma Phys.* **15** 659
[11] Garbet X *et al* 1991 *Nucl. Fusion* **31** 967